

Effects of temper condition and post weld heat treatment on the microstructure and mechanical properties of friction stir butt-welded AA7075 Al alloy plates

Güven İpekoğlu · Seçil Erim · Gürel Çam

Received: 27 May 2013 / Accepted: 11 August 2013 / Published online: 30 August 2013
© Springer-Verlag London 2013

Abstract In this study, AA7075-O and AA7075-T6 Al alloy plates were friction stir butt welded using two sets of weld parameters in order to investigate the effects of temper condition prior to joining and post weld heat treatment on microstructure and mechanical properties of the joints. Another goal of the work is to determine the possibility of restoring the loss of strength in the joint area experienced in welding of this alloy in the age-hardened condition by subsequent heat treatment. The study revealed that the friction stir welding resulted in a strength undermatching when the alloy joined in T6 condition while a significant strength overmatching was obtained in the joints produced in O temper condition. The post weld heat treatment led to a significant recovery in the strength of the joints produced in T6 condition, thus a significant increase in the joint performance. On the other hand, it led to a decrease in the joint performance value of the joints produced in O temper condition although the strength was increased. Furthermore, the post weld heat treatment resulted in abnormal grain growth in the joint area the degree of which depends on weld parameters used and the prior temper condition.

Keywords Al alloys · Friction stir welding · Temper condition · Post weld heat treatment · Abnormal grain growth

1 Introduction

Al alloys, particularly AA7075, are widely used in transport applications including aerospace industry owing to their superior specific strength and formability. However, there are

several difficulties in joining of AA7075 Al alloy in the age-hardened state, particularly in fusion joining, such as porosity formation, solidification cracking and significant strength loss in the joint area [1–5]. Friction stir welding (FSW), which is a solid state joining technique, can be used to produce sound joints in Al alloys [6–10]. Thus, several investigations have been conducted in last two decades on FSW of several Al alloys, which indicate that the welding technique in general produces joints in Al alloys with better properties than those produced by fusion welding, for instance in AA5005, AA2024, AA6061, and AA7020 alloys [11], AA7075 alloy [12], and AA6082 alloy [13]. However, the strength loss in the joint area cannot be fully overcome even in the solid state joining of this alloy including FSW in age-hardened condition since the heat experienced by the material gives rise to dissolution/coarsening of the strengthening particles in the stir zone (SZ) and the coarsening of these particles in the heat affected zone (HAZ) [14]. The loss of strength in weld region even occurs in FSW of non-heat treatable Al alloys if the material is heavily cold-worked prior to joining and/or the heat input is sufficiently high during joining [15].

Recently, several studies have been conducted to investigate the possibility of the recovery of this strength loss by post weld heat treatment (PWHT). For instance, Sato and Kokawa [16] reported that both direct artificial aging and artificial aging following solutionizing led to an increase in the strength of the joint area of FSWed AA6063 Al alloy plates. Similarly, Chen et al. [17] also observed that artificial aging following solutionizing led to improvements in the strength of the joint area of FSWed AA2219-O Al alloy plates. Safarkhanian et al. [18] also reported that the strength in the joint area of FSWed AA2024-T4 Al alloy joints could be increased by a natural aging following solutionizing. Moreover, Aydın et al. [19] investigated the effect of several different PWHTs on the strength of the weld zone of FSWed AA2024-T4 Al alloy joints and reported that only artificial aging following solutionizing led to a significant increase in the strength and natural aging following solutionizing did result in a decrease in the strength

G. İpekoğlu · G. Çam (✉)
Faculty of Engineering, Mustafa Kemal University,
31200 İskenderun, Hatay, Turkey
e-mail: gurelcam@gmail.com

S. Erim
Faculty of Engineering, Dokuz Eylül University,
35160 Buca, İzmir, Turkey

Table 1 Chemical compositions of AA7075 Al alloy plates used in this study (wt%)

Plate	Al	Si	Fe	Cu	Mn	Mg	Cr	Zn	Ti	V	Zr	Other
7075-O	Bal.	0.12	0.24	1.46	0.03	2.48	0.19	5.61	0.03	0.01	0.01	0.02
7075-T6	Bal.	0.05	0.09	1.69	0.02	2.42	0.20	5.60	0.04	0.006	0.005	0.001 B, 0.0018 Pb, 0.004 Ni, 0.0026 Sn, 0.003 Be, 0.08 H ₂ ^a

^a Milligram of H₂ per 100 g of Al

in contrast to the findings of [18]. Furthermore, Elangovan and Balasubramanian [20] investigated the influence of different PWHTs on the strength of the weld zone of FSWed AA6061-T6 Al alloy joints and reported that direct artificial aging without solutionizing led to an increase in strength whereas artificial aging following solutionizing resulted in a decrease. On the other hand, a more recent work by İpekoğlu et al. [21] demonstrated that an increase in the strength of the FSWed AA6061-T6 Al alloy joints in the weld zone could be obtained by artificial aging following solutionizing.

There are also very few studies reported on the effect of PWHT on the joint properties of 7XXX series Al alloys in the literature with contradicting results. For instance, Singh et al. [22] reported that artificial aging following solutionizing led to a decrease in the strength of the weld zone of FSWed AA7039 Al alloy joints whereas in a more recent work [23], it was observed that direct aging without solutionizing (natural or artificial aging) improved the mechanical properties of the same alloy. On the other hand, Mahoney et al. [24] reported that a direct artificial aging without solutionizing did not alter the yield stress, but decreased the tensile strength of the FSWed AA7075-T651 Al alloy plates.

It can be clearly seen from the discussion above that there are contradicting results in the literature on the influence of PHWT on the mechanical properties of FSWed Al alloys. Moreover, the work conducted on the effect of PWHT on the mechanical properties of FSWed 7XXX series Al alloys (namely AA7039 and AA7075-T651) are very limited [13, 22, 23], and there is only one work in the open literature in

which an increase in the strength could be achieved in FSWed AA7039 alloy joints [23]. Furthermore, there is no report in open literature demonstrating that the strength can be increased in the weld zone of FSWed AA7075 Al alloy, particularly in the age-hardened grade (i.e., T6). Thus, it is of interest to demonstrate that the strength loss taking place in the weld zone of this alloy (AA7075-T6) during FSW can be recovered by PWHT and that there is certainly a need for a systematic investigation on this issue. This was the motivation to conduct the current study.

The possibility of increasing the joint performance of FSWed AA7075 Al alloy joints by PWHT was investigated

Table 2 Weld parameters used

Plate	Parameters		
	Rotation rate (rpm)	Travel speed (mm/min)	Symbol
AA7075-O	1,000	150	1000/150
	1,000	150	1000/150-PWHT
	1,500	400	1500/400
	1,500	400	1500/400-PWHT
AA7075-T6	1,000	150	1000/150
	1,000	150	1000/150-PWHT
	1,500	400	1500/400
	1,500	400	1500/400-PWHT

PWHT specimens which were post weld heat treated after the joining

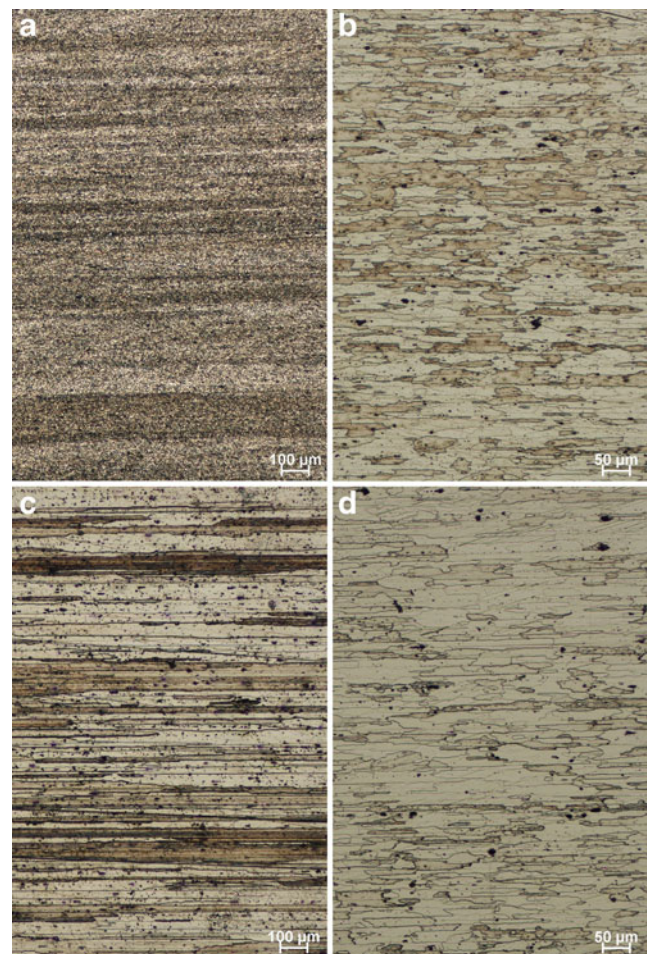
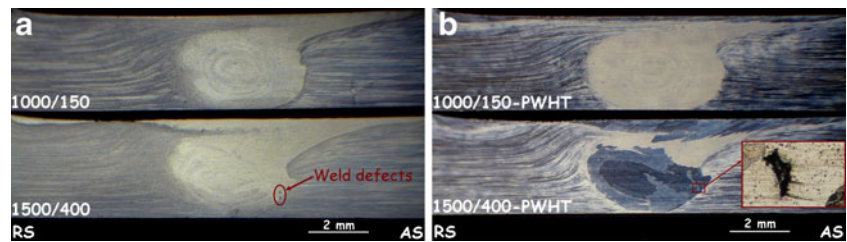


Fig. 1 Microstructures of the base plates used in this study, namely AA7075-O and AA7075-T6 Al alloys, both in the as-received and T6-treated conditions: **a** 7075-O, **b** 7075-T6, **c** T6-treated 7075-O (7075-O-HT), and **d** T6-treated 7075-T6 (7075-T6-HT)

Fig. 2 Cross-sections of the joints produced in AA7075-O Al alloy plates (O joints): **a** as-welded and **b** PWHTed



in this study. AA7075 Al alloy plates were received in two different temper conditions, namely, O and T6. Thus, the effect of the prior temper condition on the joint quality was also investigated in conjunction with the influence of PHWT.

2 Experimental procedure

2.1 Materials and specimen preparation

In this study, AA7075-O and AA7075-T6 Al alloy plates with a thickness of 3.17 mm, the chemical compositions of which are given in Table 1 [24], were used. Blanks of 300×130 mm were extracted from the plates received by laser cutting to be used in welding trials. The surfaces of the blanks were mechanically cleaned prior to joining.

2.2 Welding trials and post weld heat treatment

Welding trials were made on these blanks of 300×125 mm perpendicular to the direction of rolling, the length of welds being 300 mm. The welds were performed by using a universal CNC vertical machining center with a motion sensitivity of 1 μm and employing the usual clamping and steel backing

plate. A stirring tool with a M4-threaded cylindrical pin (its length being 3 mm) was used. The tool had a concave shoulder with a diameter of 15 mm. It was made of AISI H13 hot work steel and heat treated to a hardness of 52 HRC after machining to increase its wear resistance [21, 24, 25]. The welding trials were conducted in position control mode and no tilting of the stirring tool was employed.

Friction stir-welded joints were produced using two different sets of weld parameters for both plates (i.e., O and T6 treated), namely 1,000 rpm and 150 mm min⁻¹ (hereafter, designated as 1000/150) and 1,500 rpm and 400 mm min⁻¹ (hereafter designated as 1500/400). The former parameter set was determined to be optimum in a previous study for AA7075 plates both in O and T6 temper conditions for the experimental setup used [24] and the latter being optimum for AA6061 plates both in O and T6 temper conditions [25]. Thus, the possibility of using weld parameters, which were found to be optimum for a lower strength Al alloy (i.e., AA6061), in other words the use of a higher welding speed for this higher strength Al alloy plates (i.e., AA7075), was also investigated. A total of eight welded joints were produced on both AA7075-O and AA7075-T6 plates (hereafter designated as O joints and T6 joints, respectively) using the weld parameters of 1000/150 1500/400, Table 2. As seen from the table, two sets of joints

Fig. 3 Micrographs of the DXZs of AA7075-O joints: **a** as-welded and **b** PWHTed

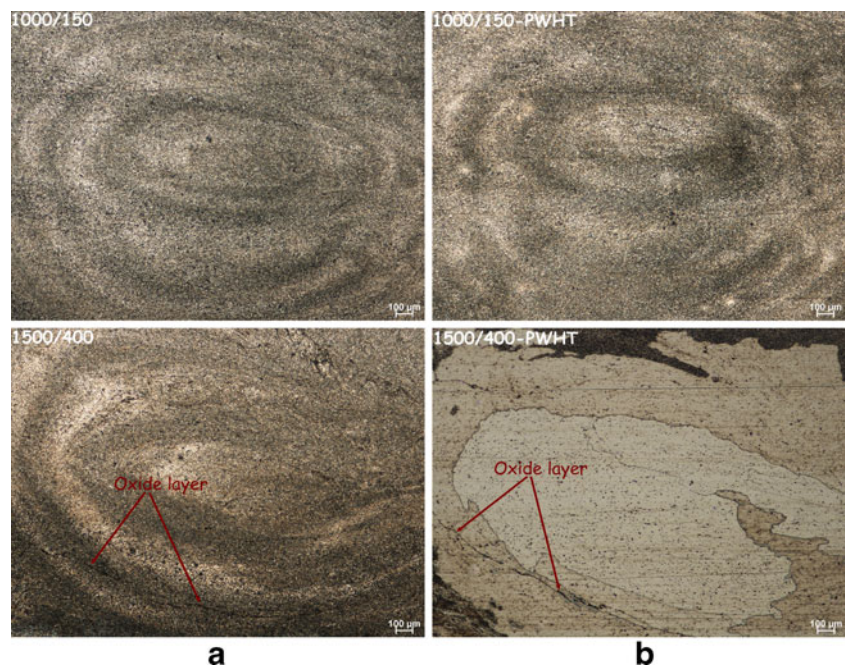
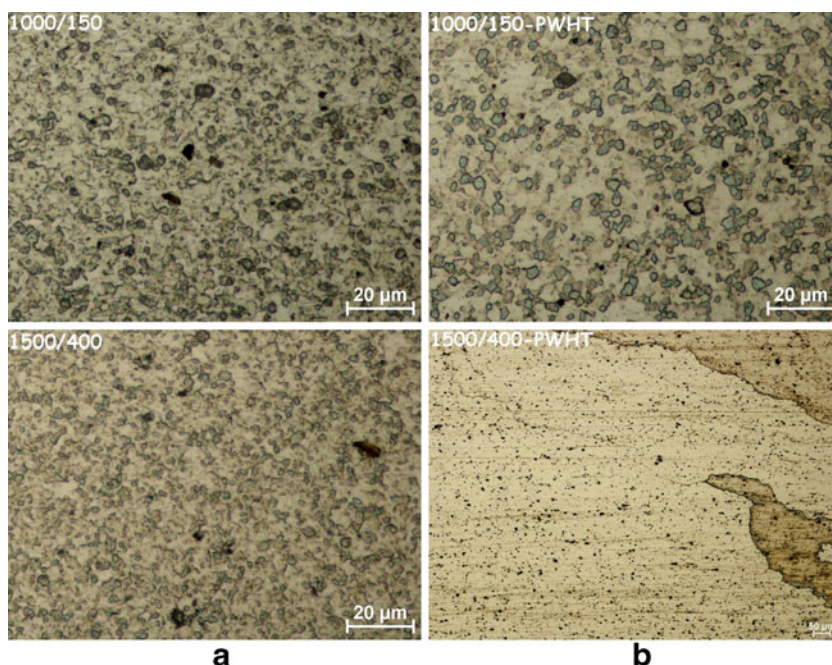


Fig. 4 Higher magnification micrographs showing DXZs of 7075-O joints: **a** as-welded and **b** PWHTed



were produced for each plate condition and parameter set in order to determine the microstructural evolution in weld zone and joint properties in the as-welded and PWHTed conditions. PWHT consisted of solutionizing at 485 °C for 4 h followed by quenching and artificial aging for 6 h at 140 °C.

2.3 Testing and characterization of joints

Four standard tensile test specimens with a gauge length of 100 mm (according to TS 287 EN 895) were extracted from each joint by electro-discharge machining. The specimens were extracted perpendicular to the weld direction, thus parallel to the rolling direction [24, 25]. Tensile tests were conducted using a universal tensile machine with a load capacity of 100 kN. All tensile tests were conducted using a loading rate of 1 mm/min.

Metallography specimens were also extracted from each joint for microstructural investigations. Following grinding and polishing, the O joint specimens were etched using a solution of 10 g NaOH and 90 ml distilled water at 65 °C

for 45 s and then the surfaces were rinsed using a solution of 50 ml HNO₃ and 50 ml distilled water for 2–4 s. On the other hand, the T6 joint specimens were etched using Keller's reagent (150 ml distilled water, 3 ml HNO₃, 6 ml HCl and 6 ml HF) at 0 °C for 25 s. A detailed investigation was carried out on the cross-section of each joint in addition to the base plates by optical microscopy to determine the microstructural evolution and also the existence of any weld defects in the joints. Furthermore, Vickers microhardness measurements were also carried out on these specimens along the centerline across the joint using a load of 100 g (loading time is 20 s).

3 Results and discussion

3.1 Microstructural aspects

Figure 1 illustrates the microstructures of the base plates used in this study, namely, AA7075-O and AA7075-T6 Al alloys, both in the as-received and T6-treated conditions. T6 aging

Fig. 5 Higher magnification micrographs of the weld areas of PWHTed 7075-O joints: **a** the transition area between SZ and base plate of the 1000/150 joint, and **b** the DXZ of 1500/400 joint. Note localized AGG formation in the shoulder area in **a** and extended AGG formation in **b**

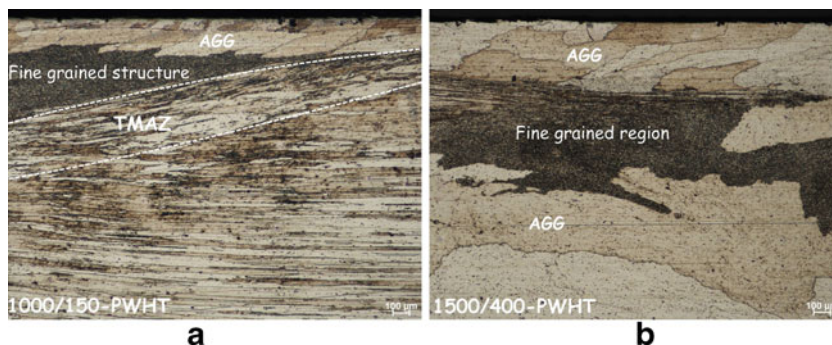
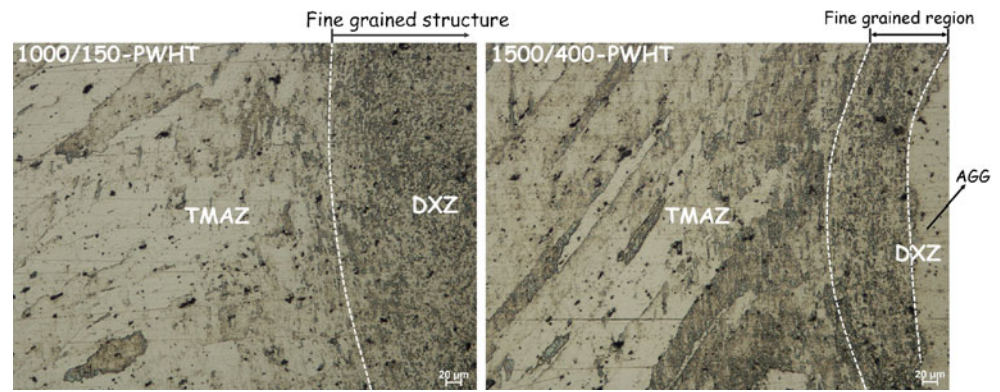


Fig. 6 Micrographs showing the microstructural evolution in the SZ of the O joints upon PWHT



treatment applied to the base plates is the same to the one used as PWHT to the welded plates. AA7075-O as-received plates exhibited a microstructure consisting of significantly elongated alpha grains indicating that it was heavily rolled (Fig. 1a). Similarly, a significantly elongated grain structure was also exhibited by the same plate after the post weld aging treatment (Fig. 1c). 7075-T6 plates also displayed an elongated grain structure in the as-received condition. However, the elongated grains in this plate were much shorter than those observed in 7075-O plates. This indicates that the degree of forming applied to 7075-O plates was higher. Moreover, undesirable inhomogeneously distributed iron- and silicon-rich particles in the form of coarse constituent particles, i.e., Al_7Cu_2Fe , $Al_{12}Fe_3Si$, and Mg_2Si , are also present in the microstructure [26]. The strengthening phases which yield the high strength of this alloy after aging are fine $MgZn_2$ precipitates homogeneously distributed in alpha grains, which are not seen in the optical micrographs given in Fig. 1b–d, since these particles are too fine and can only be resolved in transmission electron microscopy [27].

3.1.1 Microstructural aspects of O joints

Figure 2a shows the cross-sections of the joints produced in O temper condition (hereafter designated as O joint) in the as-welded condition. As seen from this figure, the joint produced with the parameter set of 1000/150 exhibited no weld-defect whereas a low amount of weld defect was observed in the SZ of the 1500/400 joint. Moreover, the presence of weld defect is also clearly seen in a higher magnification micrograph of the joint after PWHT, Fig. 2b. These results indicate that the weld parameters suitable for lower-strength AA6061 plates [25] are

not convenient for this higher-strength AA7075 Al alloy plates. This result suggests that the joint quality of FSWed higher strength AA7075-O plates is more sensitive to the weld parameters used during FSW.

Moreover, an oxide layer was also observed in the dynamically recrystallized zone (DXZ) of the 1500/400 joint both in as-welded and PWHTed conditions, Fig. 3, possibly due to the higher welding speed used in producing this joint. This in turn results in insufficient deformation to break up the oxide layer during FSW. Similarly, the presence of oxide layer was also reported for FSWed AISI 304 stainless steel joints [28].

A fine-grained microstructure was formed in the DXZs of all O joints produced, Fig. 4a, since FSW is a process in which the material deforms excessively [29, 30]. Moreover, a finer-grain structure was formed in the DXZ of the O joint produced with the parameters of 1500/400 than in that of the 1000/150 O joint.

PWHT resulted in excessive grain growth in the DXZs of both O joints, known as abnormal grain growth (AGG) [31]. Both joints exhibited a DXZ consisting of two different regions, namely AGG and fine-grained regions, Figs. 5 and 6. However, the degree of AGG formation after PWHT was quite different in two joints produced with different weld parameter sets. The extent of AGG formation was very limited in the 1000/150 joint in which the fine-grain structure evolved during FSW did not alter almost all over the cross-section of the joint except a narrow region under shoulder, Figs. 2b, 3b, 4b, and 5. In contrast, the 1500/400 joint exhibited AGG formation almost all over the cross-section, Figs. 2b, 3b, 4b, and 5.

This difference in the degree of AGG can be explained by the amount of plastic deformation (i.e., the stored energy) during FSW. If the plastic deformation is higher in some

Fig. 7 Cross-sections of the joints produced in AA7075-T6 Al alloy plates (T6 joints): **a** as-welded and **b** PWHTed

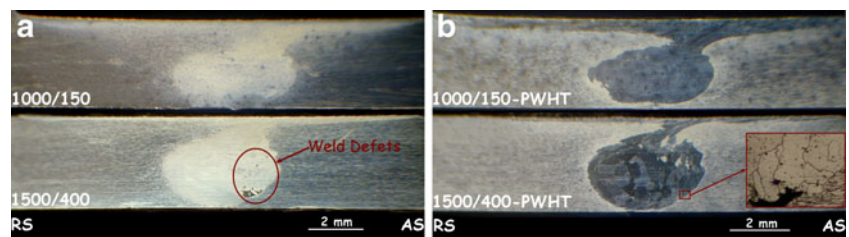
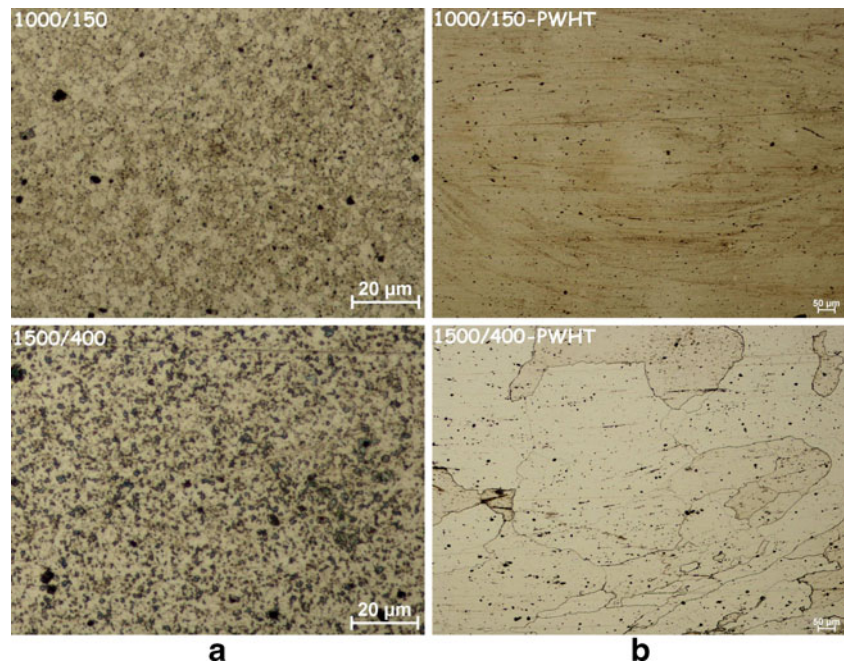


Fig. 8 Higher magnification micrographs showing DXZs of 7075-T6 joints: **a** as-welded and **b** PWHTed



regions of the weld cross-section, i.e., in the shoulder zone, AGG formation is more likely to develop in these regions. This is likely the reason for the AGG formation in a narrow region under the shoulder in the 1000/150 O joint. Moreover, the energy stored in the SZ increases as finer grains are formed. The degree of AGG formation upon subsequent heat treatment is higher when the stored energy is high [21, 31, 32]. Thus, a higher amount of AGG formation in the 1500/400 O joint after PWHT is probably due to the evolution of finer grains in the SZ prior to PWHT, Figs. 2b, 3b, 4b, and 5. This clearly indicates that the weld parameters play an important role on the degree of AGG formation upon PWHT. Similarly, Attallah and Salem [32] also reported that the weld parameters had a significant effect on AGG formation upon PWHT in FSWed AA2095 plates.

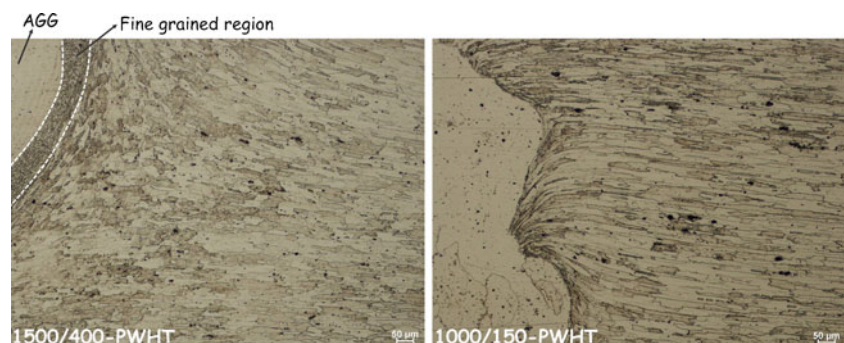
3.1.2 Microstructural aspects of T6 joints

Figure 7a shows the cross-sections of the joints produced in T6 temper condition in the as-welded condition. As seen from

this figure, the T6 joint produced with the parameter set of 1000/150 exhibited no weld-defect whereas a low amount of weld defect was observed in the SZ of the joint obtained with the parameter set of 1500/400. These results indicate that the weld parameters suitable for lower strength AA6061 plates are not convenient for this higher strength AA7075 Al alloy plates in the T6-treated condition as the case in the O joints.

As the case in the as-welded O joints, a fine-grained microstructure was formed in the DXZs of both T6 joints produced, Fig. 8a. As seen from this figure, the grain size was quite similar in both joints. However, the joint produced with the parameters of 1500/400 contain more coarse particles in the DXZ than the 1000/150 joint. Moreover, PWHT resulted in significant AGG formation in DXZs of both T6 joints (Fig. 7b), in contrast to the O joints where the degree of AGG formation was observed to be very limited in the 1000/150 O joint. However, the grain size after the AGG formation upon PWHT was different in the T6 joints produced with weld parameters of 1000/150 and 1500/400. The grain coarsening in the DXZ of 1000/150 joint was much higher

Fig. 9 Micrographs showing the microstructural evolution in the SZ of the T6 joints upon PWHT



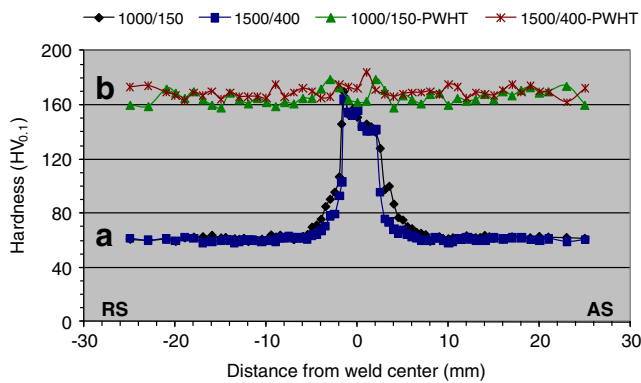


Fig. 10 Hardness profiles of AA7075-O joints both in the as-welded and PWHTed conditions

than that in the DXZ of 1500/400 joint, which is probably due to the distinct microstructure in the DXZ of this joint consisting of intermixed fine and coarse grains (probably giving rise to a higher stored energy), Figs. 7b and 8b.

It is also worth noting that the fine-grained structure evolved during FSW remained unchanged in a narrow region in the DXZ neighboring TMAZ of 1000/150T6 joint whereas the AGG formation took place all over the cross section of 1500/400T6 joint, Fig. 9, in contrast to the O joints where this narrow region was observed in the 1500/400 joint.

3.2 Hardness

Hardness profiles of O and T6 joints both in as-welded and PWHTed conditions are shown in Figs. 10 and 11, respectively. As seen from Fig. 10, the as-welded O joints displayed a hardness increase in the weld area (i.e., strength overmatching) and the maximum hardness being about 170 HV, which is 110 HV higher than that of the O temper base plate (i.e., 60 HV). Moreover, it is also worth noting that the width of the area where hardness increased after FSW is larger in the O joint produced with the weld parameter set of 1000/150. This hardness increase in the weld area is possibly due to the fact

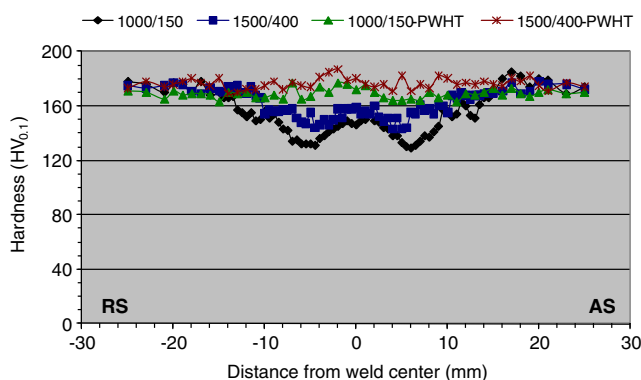


Fig. 11 Hardness profiles of AA7075-T6 joints both in the as-welded and PWHTed conditions

that the grain refinement took place in the SZ during FSW (Fig. 4). Furthermore, the O temper alloy does not usually experience a hardness loss in joining since it is annealed, i.e., soft. Similar results were also reported for FSWed AA2219-O [17]. After PWHT, the hardness profile of these joints became quite homogeneous across the joint area (i.e., strength evenmatching). The hardness was about 170 HV all over the specimen across the joint, which is slightly below the hardness usually achieved in this alloy by T6 treatment.

As seen from Fig. 11, the as-welded T6 joints displayed a hardness decrease in the weld area (i.e., strength undermatching) in contrast to the O joints where a strength overmatching was obtained. This hardness loss can be attributed to the dissolution of strengthening particles, which precipitated after T6 treatment (i.e., aging) of this alloy, in the SZ and coarsening of the strengthening particles in the HAZ. It is also worth noting that the hardness minimum lies in the HAZ region. Similar results were also reported for other Al alloy plates in T6 temper condition [14, 19–23]. The hardness profiles also showed that the degree of hardness loss in the weld area of T6 joints was higher in the joint produced using the parameters of 1000/150, the minimum hardness being 130 HV, than that observed in the 1500/400 joint, i.e., 143 HV. This is probably due to the presence of less coarse particles in the DXZ of this joint compared to that of the joint produced with the parameters of 1500/400.

Moreover, PWHT almost fully recovered the hardness loss in both T6 joints and their hardness profiles became quite homogeneous across the joint area (i.e., strength evenmatching) as the case in the O joints. However, the average hardness value obtained in the 1000/150 joint (i.e., 165 HV) was slightly lower than that of the 1500/400 (i.e., 170 HV). These hardness values are at the level of the hardness usually achieved in this alloy by T6 treatment, indicating that PWHT (i.e., T6 treatment) restores the strength in the weld area of FSWed AA7075-T6 plates to that of the respective base plate.

3.3 Tensile strength

The results of the tensile tests conducted on the base plates and the FSWed O and T6 joints, both in as-welded and PWHTed conditions, are summarized in Table 3. It gives the proof stress, tensile strength, and elongation values of the base plates and the joints. The joint performance values of the joints in terms of proof stress, tensile strength, and elongation are also given. These joint performance values were calculated using the average values for each case. Moreover, the performance values of the joints in as-welded condition were calculated using the properties of the respective base plates (as-received O or T6-treated base plates) whereas this calculation was made using the properties of as-received T6-treated base plate for all PWHTed joints. The average values obtained from the tensile tests were also presented as column graphics in Fig. 12.

Table 3 Summary of tensile test results of the base plates and the joints

Specimen	AA7075-O						AA7075-T6					
	1	2	3	4	Ave. ^a	JP (%) ^b	1	2	3	4	Ave. ^a	JP (%) ^b
Base plate												
Tensile strength, R_m (MPa)	203.2	206.8	197.2	206.6	203.5	–	563.1	559.2	567	564.7	563.5	–
Proof stress, $R_{p0.2}$ (MPa)	85.1	84.6	87	84.3	85.2	–	493.9	492.2	502	496.2	496.1	–
Elongation (%)	19.1	20.4	17.8	18.3	18.9	–	16.4	14.4	16.3	17.1	16.1	–
1000/150												
Tensile strength, R_m (MPa)	203.9	203.7	203.7	204.1	203.9	100.2	449.7	449.2	443	457.5	449.9	79.8
Proof stress, $R_{p0.2}$ (MPa)	88	89.4	88.5	87.8	88.4	103.8	365.1	364.9	369.3	365.2	366.1	73.8
Elongation (%)	14.21	14.07	13.76	14.27	14.1	74.6	1.92	1.92	1.69	1.02	1.54	9.6
1500/400												
Tensile strength, R_m (MPa)	205.7	205.8	206.1	206.2	206	101.2	380	395.8	380	372.4	382.1	67.8
Proof stress, $R_{p0.2}$ (MPa)	89.3	89.4	89.6	89.4	89.4	104.9	–	–	–	–	–	–
Elongation (%)	14.76	14.32	14.93	16.25	15.1	79.9	0.64	0.68	0.62	0.6	0.64	4
1000/150-PWHT												
Tensile strength, R_m (MPa)	506.6	539.6	538.9	515.4	525.2	93.2 ^c	508.2	521.4	485.6	492.8	502	89.1
Proof stress, $R_{p0.2}$ (MPa)	482.9	493.5	490.5	492.6	489.9	98.8 ^c	479	481.3	480.4	478.5	479.8	96.7
Elongation (%)	1.45	12.1	10.61	2.46	6.66	41.4 ^c	2.09	3.45	1.24	1.31	2.02	12.5
1500/400-PWHT												
Tensile strength, R_m (MPa)	–	490.6	497.9	491.3	493.3	87.5 ^c	458.4	524.2	535.5	529.3	511.9	90.8
Proof stress, $R_{p0.2}$ (MPa)	–	488.5	489.3	489.1	489	98.6 ^c	–	504.2	502.8	500.1	502.4	101.3
Elongation (%)	–	1.02	1.25	1.12	1.13	7 ^c	0.72	1.85	3.11	2.47	2.09	13

^a Average value

^b Joint performance value, JP=(Property of the joint/Property of respective base plate)×100,

^c Joint performance values were calculated using the properties of as-received 7075-T6 base plate.

3.3.1 Tensile strength of O joints

All traverse tensile specimens extracted from both O joints produced with the parameters of 1000/150 and 1500/400 failed in the base plate away from the joint region. These

results are in good agreement with the hardness profiles of these joints (Fig. 10), which all exhibited strength over-matching in the joint region. Moreover, even the presence of some defects and oxide layer in the SZ did not change the fracture location in traverse tensile test specimens due to the

Fig. 12 Column graphics showing the average values of the tensile properties of the base plates and the joints

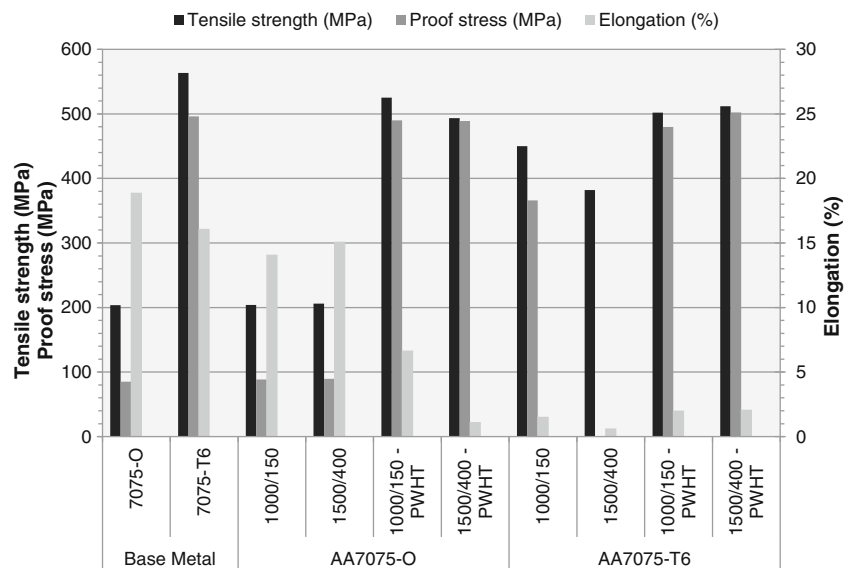
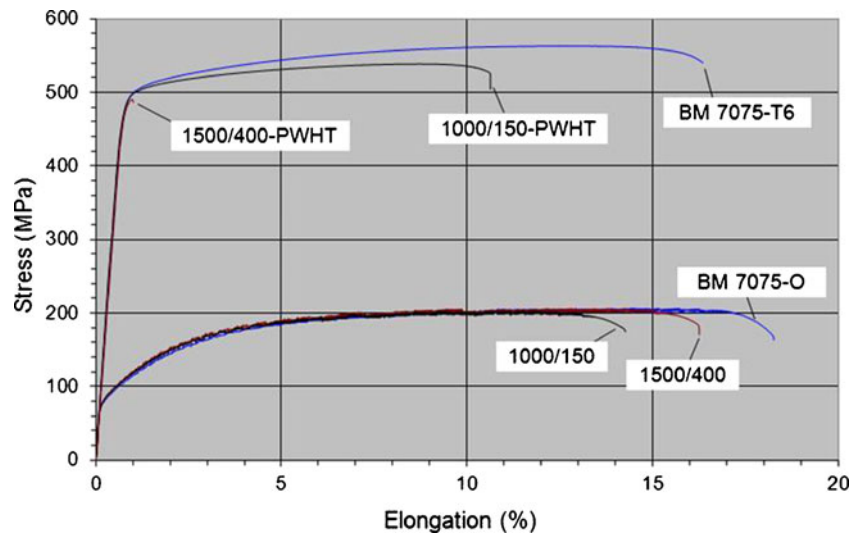


Fig. 13 Comparison of stress-elongation (in percent) curves of O joints to those of the as-received O and T6 base plates



strength overmatching, i.e., so-called shielding effect (Figs. 2 and 3).

The strength properties of these joints (i.e., proof stress and tensile strength) were similar to those of the as-received O-base plate, thus the joint performance values in terms of strength were about 100 %. On the other hand, the percent elongation values exhibited by these joints (i.e., about 14–15 %) were lower than that of the O-base plate (i.e., about 19 %) although all specimens failed in the base plate, (Table 3, Figs. 12 and 13). These low elongation values exhibited are due to the hardness increase in the weld regions (i.e., strength overmatching), which do not plastically deform during the testing, thus reducing the overall elongation of the specimens. In other words, the elongation values were determined by a video extensometer on a gauge length of 100 mm although the weld region (about 15 mm wide in the centerline) does not plastically deform during the test. Thus, only the base plate sections of the specimen (i.e., about 85 mm) plastically deform, leading to lower overall percent elongation values. In order to demonstrate the effect of strength overmatching on elongation value, the percent elongation values were also calculated using a gauge length of 50 mm on the specimens

after the test. The percent elongation values calculated using a gauge length of 50 mm decreased further as seen in Table 4. This is expected since the 50-mm gauge length contains less base plate section (i.e., about 35 mm wide). This result clearly demonstrates that the presence of strength overmatching in the weld region reduces the overall elongation of the specimen in the traverse tensile testing. Similarly, lower elongation values were also reported for laser beam-welded steel joints with strength overmatching weld regions [33, 34].

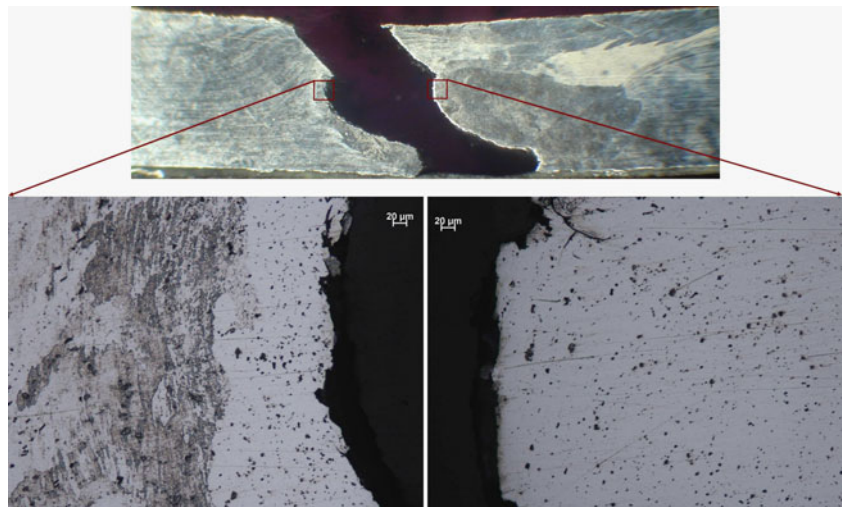
PWHT (T6 treatment) led to an increase in the strength values of both O joints (Table 3, Figs. 12 and 13). However, the 1000/150 O joint exhibited a higher tensile strength (i.e., 525 MPa) than that of the 1500/400 O joint (i.e., 493 MPa) after PWHT although the proof stress values were very similar (i.e., about 490 MPa). The highest joint performance values were obtained from the 1000/150-PWHT specimens, being about 93 % in terms of tensile strength and about 99 % in terms of proof stress. Moreover, it also exhibited a significantly higher elongation value (i.e., about 7 %) than that of the 1500/400 joint (i.e., about 1 %). The reason for the lower tensile strength and very low elongation exhibited by the PWHTed 1500/400 joint is the presence of oxide layer rather than the presence of weld defect in the DXZ of this joint (Fig. 3). This was clearly demonstrated by the fractography conducted on the 1500/400-PWHT specimens after testing (Fig. 14), in which the fracture took place along the oxide layer existing in the DXZ. The presence of oxide layer did not have any effect on the mechanical behavior of the same joint in the as-welded condition as discussed above since the weld defects were shielded by the presence of strength overmatching. Thus, the subsequent T6 treatment after joining diminishes the shielding effect created by strength overmatching since it results in a homogeneous strength distribution all over the specimen across the joint area (i.e., strength evenmatching). This indicates that PWHT can be used to increase the properties of the O joints of this alloy

Table 4 The effect of gauge length on the elongation (in percent) values of as-welded O and T6 joints

Specimen	Elongation (%)			
	7075-O		7075-T6	
	L=100 mm	L=50 mm	L=100 mm	L=50 mm
1000/150	14.1	8.65	1.54	3.75
1500/400	15.1	9.7	0.64	0.75

L gauge length

Fig. 14 The fracture location in the tensile test specimen extracted from the 1500/400 O joint after PWHT



provided that they do not contain any weld defect in the SZ prior to PWHT.

Moreover, the average elongation value of the 1000/150-PWHT joint (i.e., about 7 %) was also significantly below that of the as-received T6 base plate (i.e., 16 %) although it exhibited comparable strength values (Table 3, Figs. 12 and 13). Four specimens extracted from this joint were tested, two of which failed from the base plate away from the joint area exhibiting an elongation of about 11–12 % while the other two specimens fractured in DXZ displaying very low elongation values (namely 1.5 and 2.5 %), thus reducing the average value to about 7 % which corresponds to a joint performance value of about 41 %. The reason for this can be the fact that the welding trials were conducted by position control leading to local variations in the weld quality. The higher elongation values exhibited by the specimens failing in the base metal (i.e., about 11–12 %) were also below that of the as-received T6 base plate (i.e., 16 %), which is likely to the difference in the chemical composition, Table 1, and the degree of forming

in these two as-received base plates (namely O and T6 base plates), Fig. 1. Another reason for this difference observed in elongation values can be the difference between T6 treatments applied to the as-received T6 base plate by the supplier and the one conducted in this work.

3.3.2 Tensile strength of T6 joints

All traverse tensile specimens extracted from both T6 joints in the as-welded condition failed in the joint region in contrast to the O joints. However, the T6 joint produced using the weld parameters of 1000/150 exhibited higher strength values (i.e., proof stress and tensile strength of 382 and 450 MPa, respectively) than those of the joint produced using the parameters of 1500/400 (suitable parameters for lower strength AA6061), Table 3, Figs. 12 and 15. The reason for lower strength values exhibited by 1500/400T6 joint is the presence of weld defects in the SZ of this joint (Fig. 7). It was also observed that the specimens extracted from this joint failed in elastic region

Fig. 15 Comparison of stress-elongation (in percent) curves of T6 joints to that of the as-received T6 base plate

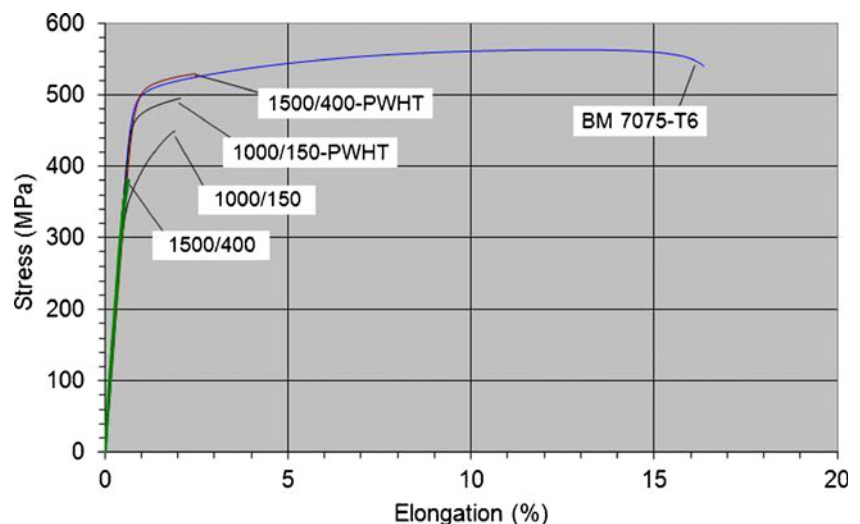
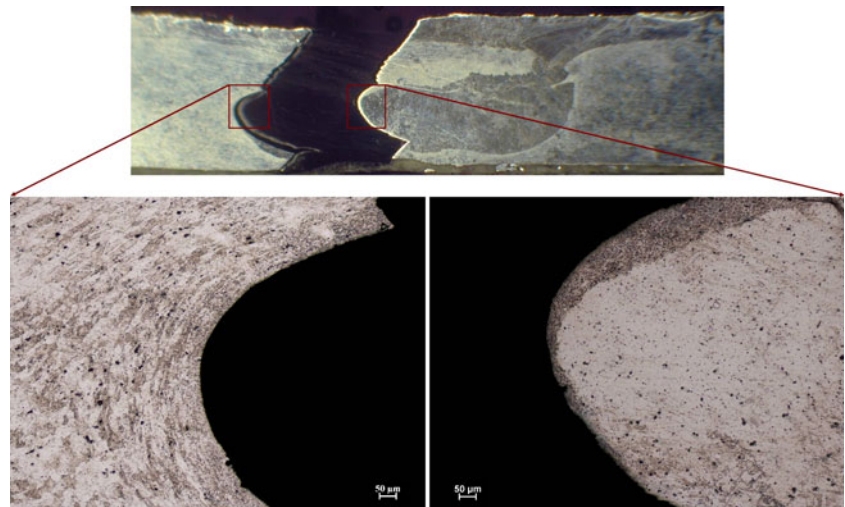


Fig. 16 The fracture location in the tensile test specimen extracted from the 1000/150 T6 joint after PWHT



without exhibiting any significant plastic deformation, Fig. 15. This shows that the heat input is insufficient during FSW of the 1500/400 joint giving rise to the formation of defects. Thus the presence of weld defects in the SZ lowers the joint strength values, indicating this parameter set is not suitable. Moreover, both T6 joints displayed a very low elongation (i.e., 0.6 and 1.5 % for 1500/400 and 1000/150 joints, respectively). The reason for this low elongation is the strength undermatching in the SZ of these joints leading to confined plasticity (Fig. 11). It is also worth pointing out that the presence of weld defects in the SZ of the 1500/400 joint seems to further decrease the elongation of the joint.

In order to demonstrate the effect of strength undermatching on elongation value, the percent elongation values were also calculated using a gauge length of 50 mm on the specimens after the test in addition to 100-mm gauge length. The percent elongation values calculated using a gauge length of 50 mm increased from about 1.5 % to about 3.8 %, as seen in Table 4, (i.e., the joint performance in terms of elongation increasing to about 23 %). This is not surprising since the 50-mm gauge length contains less base plate section with a higher proof stress (i.e., about 30 mm wide), thus the ratio of the plastically deforming section to the total length of the specimen increases. This result clearly demonstrates that the presence of strength undermatching in the weld region reduces the overall elongation of the specimen in the traverse tensile testing. Similarly, lower elongation values were also reported for FSWed cold-worked AA5083 [35] and AA5086 [15] Al alloys joints, in which the plastic deformation only took place in the weld region.

Moreover, T6 joints also exhibited lower strength values than the respective base plate (proof stress and tensile strength of which are 496 and 564 MPa, respectively), even the defect-free 1000/150T6 joint (i.e., proof stress and tensile strength being 366 and 450 MPa, respectively) due to strength undermatching. Thus, highest joint performance values in

terms of proof stress and tensile strength were about 74 and 80 %, respectively.

Similar to the case in the O joints, PWHT led to an increase in the strength values of both T6 joints (Table 3, Figs. 12 and 15). However, PWHT increased only the strength of the weld region in these joints as expected in contrast to the O joints where the strength was increased both in the base plate and the weld zone. Moreover, the proof stress and tensile strength values obtained from the specimens extracted from the 1500/400-PWHT joint, which exhibited some defects in the SZ (the average values being about 502 and 512 MPa, respectively) were higher than those of the defect-free 1000/150-PWHT joint (i.e., 480 and 502 MPa, respectively), Fig. 7. One specimen out of four extracted from 1500/400-PWHT joint exhibited very low strength and elongation values (i.e., 458 MPa and 0.7 %, respectively) than the other three specimens (i.e., >512 MPa and >1.85 %, respectively), Table 3. This indicates that this joint probably contains local defects in some areas, not throughout the joint line and the metallography specimen extracted from this joint hit a region containing weld defect.

Moreover, the proof and tensile strength values exhibited by the joints after PWHT, particularly tensile strength, were also well below those of the respective base plate, i.e., 496 and 564 MPa, respectively. This can partly be attributed to the difference between T6 treatments, namely the one given to the as-received base plate by the supplier and the one applied to the joints in this study. Thus, this joint displayed a joint performance value of 89 and 97 % in terms of proof stress and tensile strength, respectively.

Moreover, the defect-free 1000/150-PWHT joint specimens also showed much lower elongation value (i.e., about 2 %) than the respective base plate (i.e., about 16 %), which is not expected due to strength evenmatching after PWHT (i.e., the strength is homogeneous all over the specimen across the joint). The reason of this very low elongation values exhibited

by this joint can be attributed to the fact that the structure of its stir zone is inhomogeneous, i.e., containing a narrow band of fine-grained region next to the TMAZ and AGG, Fig. 9. The detailed fractography conducted on the fractured specimens of this joint clearly demonstrated that the failure indeed took place along the interface between AGG region and the fine-grained region within the SZ, Fig. 16, in a possibly brittle manner, thus reducing the elongation. This is also believed to be the reason for the lower strength values exhibited by this joint in addition to the differences in T6 treatments as discussed above.

This study clearly indicated that the strength of FSWed AA7075-T6 plates, in which a significant loss of strength experienced in the weld zone after joining (i.e., high strength undermatching), can be restored almost to the level of that of T6-treated base plate by a PWHT consisting of solutionizing followed by artificial aging. However, the ductility cannot be restored to the level of base plate. This result is contradicting with the results reported for FSWed AA7039 plate by [22, 23] in which it was observed that artificial aging following solutionizing led to a decrease in the strength of the weld zone of this alloy. It was also reported that direct aging without solutionizing (natural or artificial) improved the mechanical properties [23]. The reason for these contrasting results on the effect of subsequent PWHT (i.e., consisting of artificial aging following solutionizing) on the properties of FSWed 7XXX series Al alloys is probably due to the conduction of artificial aging at higher temperatures (i.e., 165 or 190 °C) in their work than the one used in the present study (i.e., 140 °C), probably resulting in a slightly overaged condition.

4 Conclusions

In this study, it was observed that the joint quality of AA7075 Al alloy plates is very sensitive to friction stir weld parameters both in O and T6 temper conditions. However, defect-free joints can be obtained in both plates, if a suitable weld parameter set is used. A grain refinement took place in the DXZs of all the joints produced (both in O and T6 joints) due to the dynamic recrystallization, the level of which depends on the weld parameters used. A strength overmatching was obtained in the weld region of the O joints in contrast to the strength undermatching in T6 joints. The grain refinement in the DXZ of O-plates, which is strengthened by solid solution only, results in the increase of strength in that region, whereas the strength undermatching in the weld region of T6 joints occurs due to the dissolution and coarsening of the strengthening particles in these age-hardened plates. The O joints exhibited much higher joint performance values than those displayed by T6 joints, which were in good agreement with the hardness profiles of the respective joints.

PWHT resulted in an inhomogeneous microstructure containing AGG formation in the DXZ of both O and T6 joints. However, the degree of AGG formation was found to depend on the weld parameters used. Thus, the microstructure of DXZ varies from a microstructure containing a very limited AGG formation up to a one consisting of a single grain encircled with a very narrow band of fine-grained region. PWHT also resulted in a homogeneous hardness distribution across the joint area in both O and T6 joints. Moreover, PWHT led to an increase only in the strength of the weld regions of T6 joints in contrast to the O joints where the strength was increased both in the base plate and the weld zone. The PWHTed defect-free O and T6 joints (both produced with the parameters of 1000/150) exhibited similar strength performance values. However, the joint performance value in terms of elongation was quite different in these two joints after PWHT due to the difference in their microstructures. Thus, FSW this alloy in O temper condition and then applying a PWHT is more advantageous than conducting FSW in T6 temper condition and then heat treating, particularly when higher ductility levels are desired.

Acknowledgements The authors would like to express their gratitude to the Scientific Research Projects Unit of Dokuz Eylul University, Izmir, Turkey, for financing this work partially (The project number: DEÜ 2007.KB.FEN.52). The authors would also like to thank Assoc. Prof. Dr. B. Gören Kiral for her contribution to the conduction of some experiments within the project.

References

1. Çam G, Koçak M (1998) Progress in joining of advanced materials. *Int Mater Rev* 43(1):1–44
2. Cam G, Ventzke V, Dos Santos JF, Kocak M, Jennequin G, Gonthier-Maurin P (1999) Characterisation of electron beam welded aluminium alloys. *Sci Technol Weld Join* 4(5):317–323
3. Cam G, Ventzke V, Dos Santos JF, Kocak M (2000) Characterization of laser and electron beam welded Al-alloys. *Prakt Metallogr* 37(2):59–89
4. Çam G, Kocak M (2007) Microstructural and mechanical characterization of electron beam welded Al-alloy 7020. *J Mater Sci* 42:7154–7161
5. Pakdil M, Çam G, Kocak M, Erim S (2011) Microstructural and mechanical characterization of laser beam welded AA6056 Al-alloy. *Mater Sci Eng, A* 528(24):7350–7356
6. Mishra RS, Ma ZY (2005) Friction stir welding and processing. *Mater Sci and Eng R: Reports* 50(1–2):1–78
7. Nandan R, DebRoy T, Bhadeshia HKDH (2008) Recent advances in friction-stir welding—process, weldment structure and properties. *Prog Mater Sci* 53(6):980–1023
8. Threadgill PL, Leonard AJ, Shercliff HR, Withers PJ (2009) Friction stir welding of aluminium alloys. *Int Mater Rev* 54(2):49–93
9. Çam G (2011) Friction stir welded structural materials: beyond Al-alloys. *Int Mater Rev* 56(1):1–48
10. Cam G, Kocak M (1998) Progress in joining of advanced materials—part II: joining of metal matrix composites and joining of other advanced materials. *Sci Technol Weld Join* 3(4):159–175
11. Von Strombeck A, Cam G, Dos Santos JF, Ventzke V, Kocak M (2001) A comparison between microstructure, properties, and

- toughness behavior of power beam and friction stir welds in Al-alloys. Proceedings of TMS 2001 Annual Meeting Aluminum, Automotive and Joining, TMS, New Orleans, LA, pp. 249–264
12. Mahoney MW, Rhodes CG, Flintoff JG, Spurling RA, Bingel WH (1998) Properties of friction-stir-welded 7075 T651 aluminum. *Metall Mater Trans A* 29:1955–1964
 13. Cavaliere P, Squillace A, Panella FJ (2008) Effect of welding parameters on mechanical and microstructural properties of AA6082 joints produced by friction stir welding. *J of Mater Process Technol* 200:364–372
 14. Woo W, Choo H, Brown DW, Feng Z (2007) Influence of the tool pin and shoulder on microstructure and natural aging kinetics in a friction-stir-processed 6061-T6 aluminum alloy. *Metall Mater Trans A* 38A:69–76
 15. Çam G, Gucluer S, Cakan A, Serindag HT (2009) Mechanical properties of friction stir butt-welded Al-5086 H32 plate. *Mat-wiss U Werkstofftech* 40(8):638–642
 16. Sato YS, Kokawa H (2001) Distribution of tensile property and microstructure in friction stir weld of 6063 aluminum. *Metall Mater Trans A* 32A:3023–3031
 17. Chen YC, Liu HJ, Feng JC (2006) Effect of post-weld heat treatment on the mechanical properties of 2219-O friction stir welded joints. *J Mater Sci* 41:297–299
 18. Safarkhanian MA, Goodarzi M, Boutorabi SMA (2009) Effect of abnormal grain growth on tensile strength of Al–Cu–Mg alloy friction stir welded joints. *J Mater Sci* 44:5452–5458
 19. Aydın H, Bayram A, Durgun I (2010) The effect of post-weld heat treatment on the mechanical properties of 2024-T4 friction stir welded joints. *Mater Des* 31(5):2568–2577
 20. Elangovan K, Balasubramanian V (2008) Influences of post-weld heat treatment on tensile properties of friction stir-welded AA6061 aluminum alloy joints. *Mater Charact* 59(9):1168–1177
 21. İpekoğlu G, Erim S, Çam G (2013) Investigation into the influence of post-weld heat treatment on the friction stir welded AA6061 Al-alloy plates with different temper condition. *Mater Metall Trans A*, submitted for publication
 22. Singh RKR, Sharma C, Dwivedi DK, Mehta NK, Kumar P (2011) The microstructure and mechanical properties of friction stir welded Al–Zn–Mg alloy in as welded and heat treated conditions. *Mater Des* 32:682–687
 23. Sharma C, Dwivedi DK, Kumar P (2013) Effect of post weld heat treatments on microstructure and mechanical properties of friction stir welded joints of Al–Zn–Mg alloy AA7039. *Mater Des* 43:134–143
 24. İpekoğlu G, Gören Kırıl BG, Erim S, Çam G (2012) Investigation of the effect of temper condition on friction stir weldability of AA7075 Al-alloy plates. *Mater Tehnol* 46(6):627–632
 25. İpekoğlu G, Erim S, Kırıl BG, Çam G (2013) Investigation into the effect of temper condition on friction stir weldability of AA6061 Al-alloy plates. *Kovove Mater* 51(3):155–163
 26. Ayer R, Koo JY, Steeds JW, Park BK (1985) Microanalytical study of the heterogeneous phases in commercial Al–Zn–Mg–Cu alloys. *Metal Trans A* 16:1925–1936
 27. Vander Voort GF (2006) Atlas of aluminum microstructures. In: MacKenzie DS, Totten GE (eds) *Analytical characterization of aluminum, steel and superalloys*. CRC Press, New York
 28. Meran C, Canyurt OE (2010) Friction stir welding of austenitic stainless steels. *Journal of Achievements in Materials and Manufacturing Engineering* 43(1):432–439
 29. Reynolds AP (2003) Friction stir welding of aluminum alloys. In: Totten GE, Mackenzie DS (eds) *Handbook of aluminum (volume 2): alloy production and materials manufacturing*. Marcel Dekker, New York
 30. Mishra RS, Mahoney MW (2007) Introduction. In: Mishra RS, Mahoney MW (eds.). *Friction Stir welding and processing*. ASM International, Ohio
 31. Humphreys FJ, Hatherly M (2004) *Recrystallization and related annealing phenomena*. Elsevier, Oxford
 32. Attallah MM, Salem HG (2005) Friction stir welding parameters: a tool for controlling abnormal grain growth during subsequent heat treatment. *Mater Sci Eng, A* 391:51–59
 33. Cam G, Yeni C, Erim S, Ventzke V, Kocak M (1998) Investigation into properties of laser welded similar and dissimilar steel joints. *Sci Technol Weld Joint* 3(4):177–189
 34. Cam G, Erim S, Yeni C, Kocak M (1999) Determination of mechanical and fracture properties of laser beam welded steel joints. *Weld J* 78(6):193s–201s
 35. Peel M, Steuwer A, Preuss M, Withers PJ (2003) Microstructure, mechanical properties and residual stresses as a function of welding speed in aluminium AA5083 friction stir welds. *Acta Mater* 51:4791–4801